Docking Operation by Two DOF Dual Arm Planar Cooperative Space Robot

Haresh Patolia, P. M. Pathak*, S. C. Jain
Robotics and Control Laboratory
Mechanical and Industrial Engineering Department
Indian Institute of Technology, Roorkee, India, 247667

*Corresponding author (pushp_pathak@yahoo.com)

Abstract

This work presents force control in dual arm planar cooperative space robot for cooperative manipulation by two arms. A docking operation by the two arms of the space manipulator has been carried out. During docking operation, space robot requires mechanical interaction with compliant objects, which encounter force and motion constraints. The gripping force should be such that the object should not slip and at the same time there is a limit on the maximum force to prevent the object from crushing. Apart from this the docking operation requires that the gripped object follows a specific path to dock the picked object. The work uses the concept of impedance control to achieve both the objectives, i.e. force control during gripping and trajectory control during docking. The methodology has been validated with simulated results.

Keywords: Free-flying, dual arm manipulator, virtual foundation, force control

1 Introduction

Unlike ground-base robot manipulator, the space manipulator has no fixed base. The dynamic reaction forces and moments due to the manipulator motion will disturb the space robot base.

An ideal approach to control the force in robotic system is by impedance modulation strategy. Control of space robot has been studied by many authors but control studies on multi arm space robots are only few. Dubowsky *et al.* [1] discussed concepts of virtual Manipulator (VM) model with an application to workspace analysis. Papadopoulos *et al.* [2] compared by simulation study, the performance of Euler angle, Euler parameter based control law to that of a transposed Jacobian algorithm and showed that the latter gives reasonably good performance with reduced computational burden. Huang *et al.* [3] developed a space robot system consisting of two arms, with one arm (mission arm) for accomplishing the capture mission, and the other one (balance arm) compensating for the disturbance of the base. Yuan *et al.* [4] analyzed multi-arm coordinated free-flying space robot with external force acting and obtained the dynamics equation for it. Annapragada *et al.* [5] discussed the behavior of free-floating robots that are involved in the capture of satellites in space. Moosavian *et al.* [6] studied a force tracking strategy for object manipulation tasks. Kumar *et al.* [7] discussed the concept of passive degree of freedom (DOF) as virtual foundation to control the interaction force between space robot tip and environment. Deshpande *et al.* [8] presented the joint trajectory planning of dual arm space robot. Pathak *et al.* [9] discussed impedance control of space robots using passive degrees of freedom in controller domain. Kumar *et al.* [10] achieved modulation of virtual foundation compensation gain through a heuristic expression involving actual and limiting forces.

This work presents the strategy for docking of a floating object of unknown mass by the dual arm space robot. The docking operation involves the gripping of the floating object by two arms and then moving the object from one location to another location. A bond graph [11-12] model of a dual arm robot system has been developed. Force control has been achieved during gripping by impedance control and the trajectory control is used for docking.

2 Impedance Control in Space Robot

The impedance of the system at an interaction port is defined as the ratio between the output effort (force) and the input flow (velocity). For applications demanding high trajectory tracking accuracy, the robotic systems are programmed to have high impedance at the end-effector. This leads to poor accommodation of external disturbances during interaction, and hence control of interaction force is difficult. However, many situations demand a robotic controller to have a balance of both the characteristics, i.e. good trajectory robustness and accommodation to environment interaction forces or torques. This is achieved by controlling the impedance appropriately instead of controlling the position or the force separately.

Another issue in control of the robot manipulators is the uncertainty in the dynamic model of it. These uncertainties include unknown parameters, unknown functions, disturbances and uncontrolled dynamics. Hence, one prefers robust trajectory control strategies that make the system insensitive to various manipulator parameters and ensure bounded trajectory tracking errors. An additional DOF is incorporated in the manipulator like a flexible foundation for specific purposes. When such additional DOF are introduced in the manipulator, suitable modifications in the controller are required for the trajectory tracking robustness. Further, if these additional DOF are suitably designed and incorporated, they can be made a desired accommodation of the external disturbing forces that arise during interaction.

In case of ground robot, robot is assumed to be riding on a physical flexible foundation interacting with environment. Here the foundation is termed as existing in physical domain. Impedance controller with foundation moved to controller domain is useful for having an entirely software controlled impedance behavior at the end-effector of the robotic system. This controller is developed through a system based bond graph approach, where certain transformations are performed among the various junction structures in the multi energy domain preserving the output impedance characteristic of the robotic system.

The concept discussed for modeling a ground robot on flexible physical foundation can be used to model a space robot by replacing the flexible physical foundation with the base of space robot. The difference of a space robot from ground robot on flexible foundation can be listed as,

(i) In case of the space robot, translation as well as rotational DOF of the base is present, whereas in a ground robot on a flexible foundation, only translation DOF is present.

(ii) Non-linearities are present due to coupled motion of the translation and rotational DOF.

(iii) Additional constraints of linear and angular momentum conservation are present which leads to problem of non-holonomy in motion planning.

Hence in modeling and controller design for a space robot, the above factors are required to be taken into consideration.

Modeling of one-translation DOF space robot with impedance controller is achieved in following stages.

Stage I: Modeling of the Space Robot

The space robot is modeled by considering a translation one DOF ground robot on a flexible foundation. Next, this flexible foundation is replaced by the space vehicle carrying the space robot. To nullify the effect of the motion of space vehicle on the tip velocity of the space robot, the base velocity of space robot is fed back to the controller.

Stage II: Modeling of the Impedance Controller

The features of stage I appended to the ground robot with virtual foundation will result in a space robot on a virtual foundation which is in controller domain.

The conceived schematic model of the space robot on a virtual foundation is shown in Fig. (1). The corresponding bond graph model is shown in Fig. (2).

For this model, the admittance at the interaction point is defined as ratio of the robot tip velocity to the

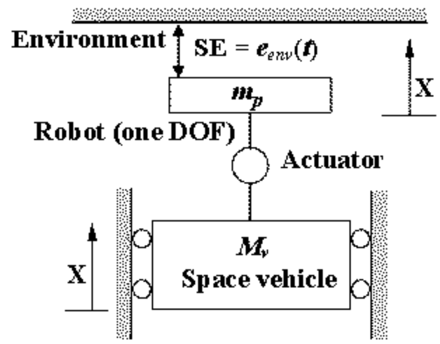

Fig. 1: Schematic diagram of one translational DOF space robot with virtual foundation in controller domain

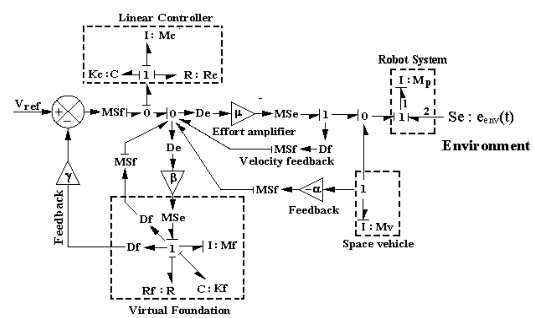

Fig. 2: Bond graph model one translational DOF space robot with virtual foundation in controller domain

environmental effort causing the motion, and can be given as [9],

$$Y_{rob}(s) = \frac{f_1}{e_2} = \frac{R(s)[1+\beta(1-\gamma)F(s)C(s)+\mu(1-\alpha)C(s)F_V(s)]}{1+\mu C(s)R(s)+\beta(1-\gamma)F(s)C(s)+\mu(1-\alpha)C(s)F_V(s)} \quad (1)$$

where,

$R(s) = 1/M_p s$ is transfer function of the robot,

$C(s) = (M_c s^2 + R_c s + K_c)/s$ is transfer function of the controller,

$F(s) = s/(M_f s^2 + R_f s + K_f)$ is transfer function of the foundation,

$F_v(s) = 1/M_v s$ and is transfer function of the space vehicle,

α = feedback compensation from space robot base to controller,

μ = high feed forward gain,

β = high gain

γ = feedback compensation from virtual foundation to controller,

At α = 1,

$$Y_{rob}(s) = \frac{R(s)[1+\beta(1-\gamma)F(s)C(s)]}{1+\mu C(s)R(s)+\beta(1-\gamma)F(s)C(s)} \quad (2)$$

From Eq. (2) it is implied that

(i) when γ = 1, the controller totally rejects the foundation characteristic and assures complete trajectory robustness,

(ii) when γ < 1, modulation of impedance to accommodate interaction forces is possible.

In the bond graph of Fig. (2), M_v is mass of the space vehicle; M_f, K_f and R_f are mass, stiffness and damping resistance respectively of the virtual foundation which is in controller domain. These values have been taken by trial and error method to achieve the control objective.

3 Modeling of Two DOF Dual Arm Planar Cooperative Space Robot

In the case of multi DOF robots, any constraint in the motion of manipulator will generate forces on the end-effector. End-effector motion can be decomposed in a local constraint frame along the normal and tangent to the constraint. In the normal direction, force needs to be controlled, while along the tangent direction robust position control is required.

The modeling of the space robot can be carried out just like a ground robot with a difference that, in case of the space robot, the base is not fixed. It involves the modeling for linear and rotational dynamics of the links and the base of space robot. In modeling of the space robot following assumptions are made,

(i) The spacecraft attitude control system is turned off when space robot is operating in a free-floating mode, and hence the spacecraft can translate and rotate in response to the manipulator movement or interaction, if any with the environment.

(ii) System has manipulator with revolute joints and is in open kinematic chain configuration.

(iii) Only planar motion of robot is considered.

(iv) The manipulator is operated at low speed, so that change in momenta which is prominent at high speed can be neglected. Thus joint efforts can be computed based on Jacobian only.

To model a two DOF dual arm cooperative space robot, first a two DOF manipulator is modeled and controller is developed. Then two such kinds of manipulators are mounted on a common base to work together. For a two DOF planar space robot, the displacement relation can be derived trigonometrically and from the

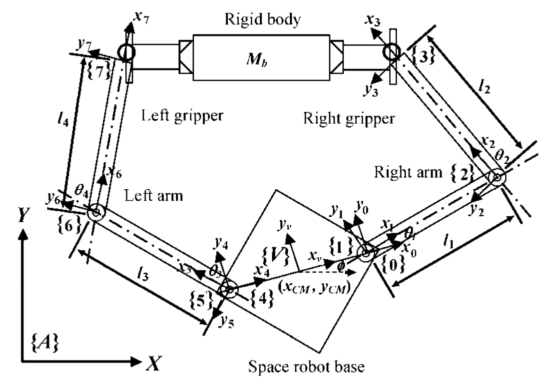

Fig. 3: Schematic diagram of two DOF dual arm planar cooperative space robot

time differentiation of these relations, the velocity relations can be derived. Fig. (3) shows the schematic diagram of a two DOF dual arm planar space robot working in cooperative mode. In Fig. (3), $\{A\}$ represents the absolute frame, $\{V\}$ represents the vehicle base frame, {0} and {4} frames are located at the base of the robot. Frames {1} and {2} are located at first and second joint of right arm and frames {5} and {6} are located at first and second joint of left arm respectively. Frame {0} coincides with frame {1} and frame {4} coincides with frame {5}. Frame {3} is located at the tip of the right arm and frame {7} is located at the tip of the left arm. Lengths of the links are assumed along the X axis of respective frames. Let l_1 and l_2 be the lengths of the first and second link of right arm and l_3 and l_4 be the length of the first and second links of left arm. Let r be the radius of the robot base.

Let ϕ represents the rotation of base frame with respect to absolute frame, and θ_1, θ_2, θ_3, θ_4 be the joint angles as shown in Fig. (3). Let X_{CM} and Y_{CM} be the coordinate of the center of mass (CM) of robot with respect to the absolute frame. The kinematic relations for the tip displacement X_{tip} and Y_{tip} of both arms of robot in X and Y directions in absolute frame can be easily found. A robot manipulator is mathematically modeled by a set of DH-parameters a_i (link length), α_i (link twist), d_i (joint distance) and θ_i (joint angle).

The bond graph model of the system is consisted of three parts. First part involves modeling of dual arm space robot, second part involves the calculation of Jacobian and the third part is modeling of the virtual foundation. All parameters of model are represented in the inertial frame.

3.1 Modeling of Dual Arm Space Robot

The kinematic relations for the tip displacement in X and Y directions for both, right and left arms of the space robot can be written as,

$$\begin{bmatrix} X_{tip} \\ Y_{tip} \end{bmatrix}_R = \begin{bmatrix} X_{CM} + rc\phi + l_1 c(\phi+\theta_1) + l_2 c(\phi+\theta_1+\theta_2) \\ Y_{CM} + rs\phi + l_1 s(\phi+\theta_1) + l_2 s(\phi+\theta_1+\theta_2) \end{bmatrix} \quad (3)$$

$$\begin{bmatrix} X_{tip} \\ Y_{tip} \end{bmatrix}_L = \begin{bmatrix} X_{CM} - rc\phi - l_3 c(\phi+\theta_3) - l_4 c(\phi+\theta_3+\theta_4) \\ Y_{CM} - rs\phi - l_3 s(\phi+\theta_3) - l_4 s(\phi+\theta_3+\theta_4) \end{bmatrix} \tag{4}$$

From Eq. (3) and (4), the velocities of the tips of the right and left arms of the space robot can be derived as,

$$\begin{bmatrix} \dot{X}_{tip} \\ \dot{Y}_{tip} \end{bmatrix}_R = \begin{bmatrix} \dot{X}_{CM} \\ \dot{Y}_{CM} \end{bmatrix} + \begin{bmatrix} -r\dot{\phi}\, s\phi \\ r\dot{\phi}\, c\phi \end{bmatrix} +$$
$$\begin{bmatrix} -l_1(\dot{\phi}+\dot{\theta}_1)s(\phi+\theta_1) - l_2(\dot{\phi}+\dot{\theta}_1+\dot{\theta}_2)s(\phi+\theta_1+\theta_2) \\ l_1(\dot{\phi}+\dot{\theta}_1)c(\phi+\theta_1) + l_2(\dot{\phi}+\dot{\theta}_1+\dot{\theta}_2)c(\phi+\theta_1+\theta_2) \end{bmatrix} \tag{5}$$

$$\begin{bmatrix} \dot{X}_{tip} \\ \dot{Y}_{tip} \end{bmatrix}_L = \begin{bmatrix} \dot{X}_{CM} \\ \dot{Y}_{CM} \end{bmatrix} + \begin{bmatrix} r\dot{\phi}\, s\phi \\ -r\dot{\phi}\, c\phi \end{bmatrix} +$$
$$\begin{bmatrix} l_3(\dot{\phi}+\dot{\theta}_3)s(\phi+\theta_3) + l_4(\dot{\phi}+\dot{\theta}_3+\dot{\theta}_4)s(\phi+\theta_3+\theta_4) \\ -l_3(\dot{\phi}+\dot{\theta}_1)c(\phi+\theta_3) - l_4(\dot{\phi}+\dot{\theta}_3+\dot{\theta}_4)c(\phi+\theta_3+\theta_4) \end{bmatrix} \tag{6}$$

In Eqs. (3) to (6), *c*( ) = *cos*( ) and *s*( ) = *sin*( ). Using Eq. (5) and (6), the different transformer moduli for the bond graph model of dual arm space robot can be derived.

3.2 Evaluation of Jacobian

As the controller works in the inertial frame and it is provided with reference velocity command in inertial frame, velocities from joint space are mapped into inertial space using the Jacobian of the forward kinematics. The difference in the reference velocity is computed and fed to the controller, which in turn provides the joint torques. The Jacobian of the forward kinematics can be calculated in bond graph as,

$$\begin{bmatrix} \textit{Tip velocity} \\ \textit{of robot} \\ \textit{with respect to} \\ \textit{absolute frame} \end{bmatrix} = \begin{bmatrix} \textit{Velocity of} \\ \textit{robot base} \\ \textit{with respect to} \\ \textit{absolute frame} \end{bmatrix} + \begin{bmatrix} \textit{Tip velocity of} \\ \textit{robot with respect} \\ \textit{to robot base} \\ \textit{due to joint motion} \end{bmatrix} + \begin{bmatrix} \textit{Linear velocity of} \\ \textit{robot tip due to} \\ \textit{angular motion} \\ \textit{of the robot base} \end{bmatrix} \tag{7}$$

All above mentioned velocities are expressed in absolute frame and in equation form, this relationship can be written as,

$$^A(^AV_3) = {}^A(^AV_0) + {}^A_0R^0(^0V_3) + {}^A_vR(-{}^v_0R^0(^0P_3) \times {}^v(^A\omega_v)) \tag{8}$$
$$^A(^AV_7) = {}^A(^AV_4) + {}^A_4R^4(^4V_7) + {}^A_vR(-{}^v_4R^4(^4P_7) \times {}^v(^A\omega_V)) \tag{9}$$

In the planar case discussed here, this relationship can be worked out directly as shown by Eq. (5) and (6). These equations are used to calculate the Jacobian as shown in Fig. (4).

3.3 Modeling of the Virtual Foundation

In order to modulate the impedance at the robot tip and environment interaction point, a virtual foundation is assumed. The foundation has a rotational compliance K_f, rotational damping resistance R_f, mass M_f and rotational inertia I_f. Drawing analogy from the space vehicle, the virtual foundation velocities in *X* and *Y* direc-

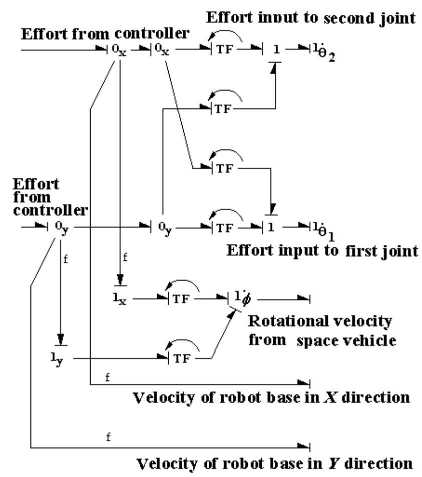

Fig. 4: Bond graph sub-model for evaluation of Jacobian

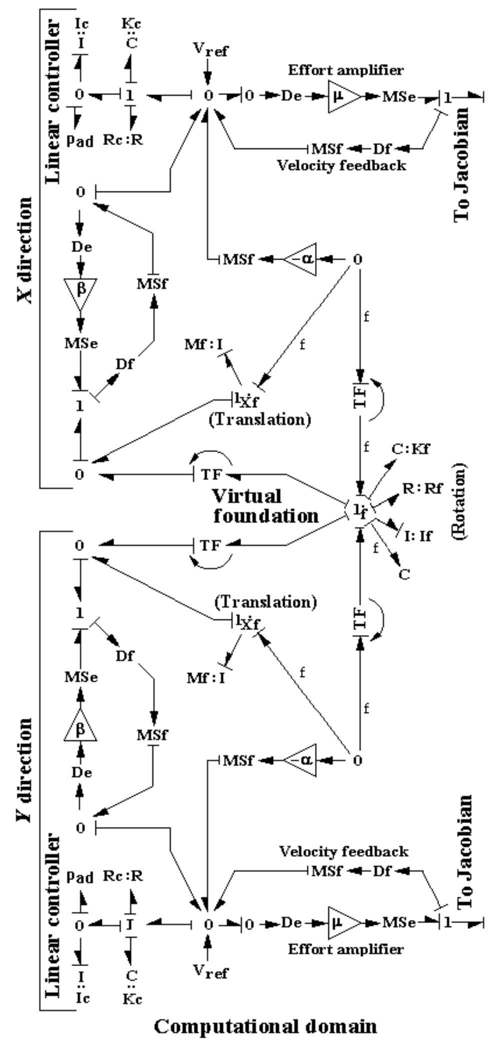

Fig. 5: Bond graph sub-model of a two DOF planar space robot controller

tion are considered. The velocities of the tips of the right and left arms of the space robot can be derived as,

$$\begin{bmatrix} \dot{X}_{tip\,f} \\ \dot{Y}_{tip\,f} \end{bmatrix}_R = \begin{bmatrix} \dot{X}_f \\ \dot{Y}_f \end{bmatrix} + \begin{bmatrix} -r\dot{\phi}_f s\phi_f \\ r\dot{\phi}_f c\phi_f \end{bmatrix} + \begin{bmatrix} -l_1(\dot{\phi}_f+\dot{\theta}_1)s(\phi_f+\theta_1) - l_2(\dot{\phi}_f+\dot{\theta}_1+\dot{\theta}_2)s(\phi_f+\theta_1+\theta_2) \\ l_1(\dot{\phi}_f+\dot{\theta}_1)c(\phi_f+\theta_1) + l_2(\dot{\phi}_f+\dot{\theta}_1+\dot{\theta}_2)c(\phi_f+\theta_1+\theta_2) \end{bmatrix} \quad (10)$$

$$\begin{bmatrix} \dot{X}_{tip\,f} \\ \dot{Y}_{tip\,f} \end{bmatrix}_L = \begin{bmatrix} \dot{X}_f \\ \dot{Y}_f \end{bmatrix} + \begin{bmatrix} r\dot{\phi}_f s\phi_f \\ -r\dot{\phi}_f c\phi_f \end{bmatrix} + \begin{bmatrix} l_3(\dot{\phi}_f+\dot{\theta}_3)s(\phi_f+\theta_3) + l_4(\dot{\phi}_f+\dot{\theta}_3+\dot{\theta}_4)s(\phi_f+\theta_3+\theta_4) \\ -l_3(\dot{\phi}_f+\dot{\theta}_3)c(\phi_f+\theta_3) - l_4(\dot{\phi}_f+\dot{\theta}_3+\dot{\theta}_4)c(\phi_f+\theta_3+\theta_4) \end{bmatrix} \quad (11)$$

Here ϕ_f is the rotation of the virtual foundation. If it is assumed that the controller overwhelms the robot dynamics, then Eq. (10) and (11) can be written as,

$$\begin{bmatrix} \dot{X}_{tip\,f} \\ \dot{Y}_{tip\,f} \end{bmatrix}_R = \begin{bmatrix} \dot{X}_f \\ \dot{Y}_f \end{bmatrix} + \begin{bmatrix} -r\dot{\phi}_f s\phi_f \\ r\dot{\phi}_f c\phi_f \end{bmatrix} + \begin{bmatrix} -l_1\dot{\phi}_f s(\phi_f+\theta_1) - l_2\dot{\phi}_f s(\phi_f+\theta_1+\theta_2) \\ l_1\dot{\phi}_f c(\phi_f+\theta_1) + l_2\dot{\phi}_f c(\phi_f+\theta_1+\theta_2) \end{bmatrix} \quad (12)$$

$$\begin{bmatrix} \dot{X}_{tip\,f} \\ \dot{Y}_{tip\,f} \end{bmatrix}_L = \begin{bmatrix} \dot{X}_f \\ \dot{Y}_f \end{bmatrix} + \begin{bmatrix} r\dot{\phi}_f s\phi_f \\ -r\dot{\phi}_f c\phi_f \end{bmatrix} + \begin{bmatrix} l_3\dot{\phi}_f s(\phi_f+\theta_3) + l_4\dot{\phi}_f s(\phi_f+\theta_3+\theta_4) \\ -l_3\dot{\phi}_f c(\phi_f+\theta_3) - l_4\dot{\phi}_f c(\phi_f+\theta_3+\theta_4) \end{bmatrix} \quad (13)$$

Eq. (12) and (13) can be used to design virtual foundation as shown in Fig. (5).

3.4 Adaptive Gain Modulation

The modulation of virtual foundation compensation gain γ through a heuristic expression involving actual and limiting forces and is given as,

$$\gamma(F, F_{\lim}, t) = 1 - swi(F(t), F_{\lim})[K_{ini} + K_{GP} * F_d + K_{GI} * Y(t)] \quad (14)$$

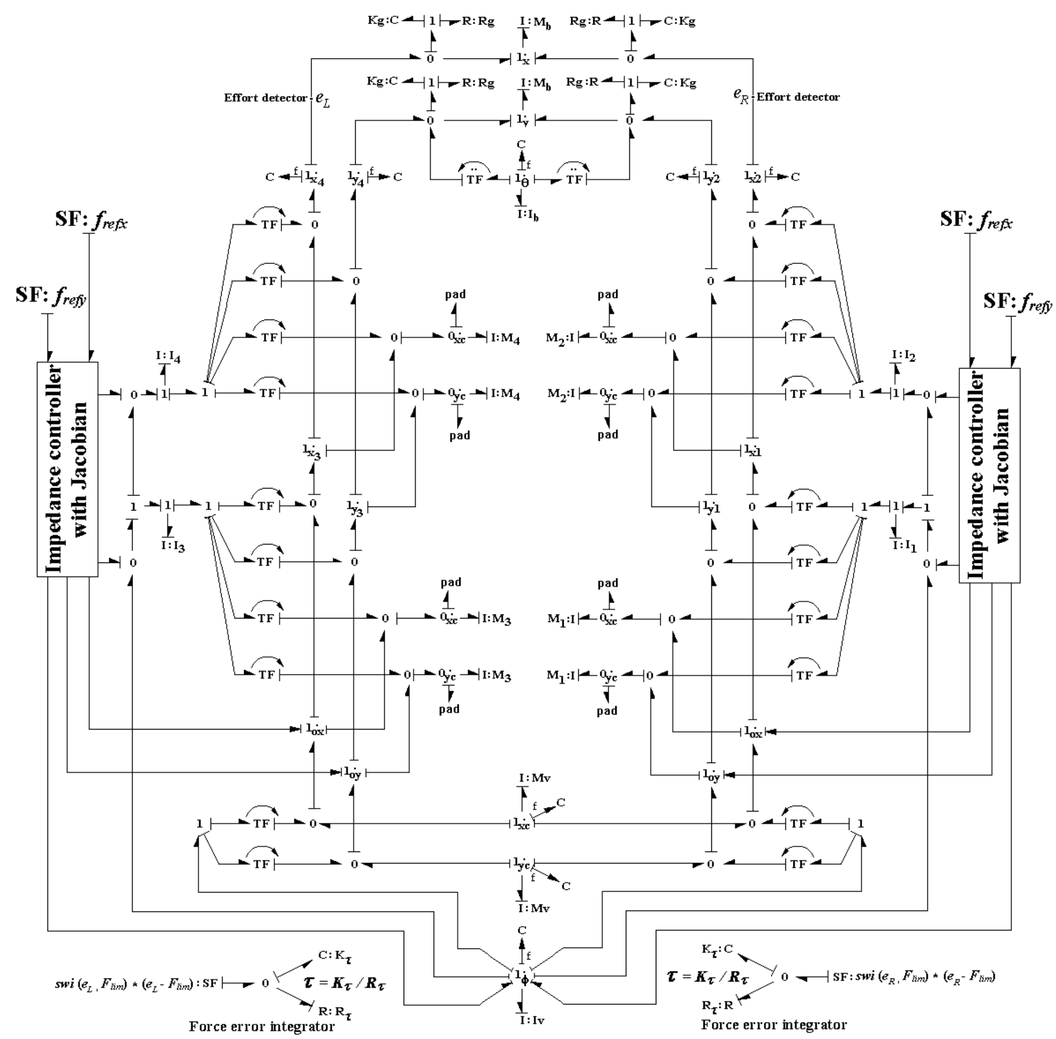

Fig. 6: Bond graph model of two DOF dual arm planar cooperative space robot

where,

$F(t)$ is the actual contact force,

F_{lim} is the limiting force,

F_d is difference between $F(t)$ and F_{lim},

K_{ini} is the constant,

K_{GP} is a proportional gain,

K_{GI} is an integral gain.

Eq. (14) represents PI control. The term $Y(t)$ is given as,

$$Y(t) = swi(F(t), F_{\lim}) * e^{-\tau t} \int_{ti}^{t} e^{\tau\xi} (F(\xi) - F_{\lim}) d\xi \quad (15)$$

Here τ is a gain relaxation term which can be calculated as shown in part bond graph of force error integrator in Fig. (6). t_i is the time when force control is initiated. The expression $Y(t)$ integrates the difference in the interaction force and the force limit to smoothen any sharp change in variation of impedance. The term *swi* defines the switch function in SYMBOLS Shakti [10,11] and it is defined as,

$swi(a,b) = 1$ if $a \geq b$ and $swi(a,b) = 0$ if $a < b$.

The complete bond graph of two DOF dual arm planar cooperative space robot is shown in Fig. (6). In this bond graph model, soft pads are used to remove differential causality from the bond graph system.

3 Simulation and Results

It is assumed that the tips of both the arms are in contact with the floating body initially which is required to be grasped first and as soon as the specified limit of forces generated by the grippers, the grasped body is docked along the given trajectory with the cooperative action of both the arms of the space robot. The initial

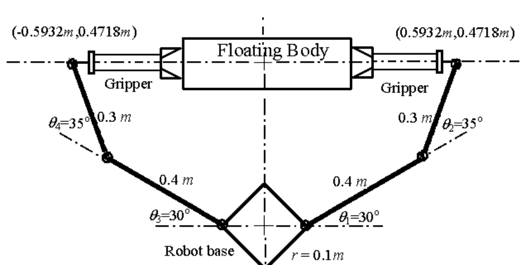

Fig. 7: Initial configuration of two DOF dual arm planar cooperative space robot

configuration of the two DOF dual arm planar cooperative space robot is shown in the Fig. (7). The form closure case has been assumed hare. The initial values for the joint angles are shown in Table I.

During the docking operation, the minimum gripping force required to be maintained is 40 *N*. The parameters and values used for simulation are shown in Table II. The simulation is performed by giving the arm tip velocities in *X* and *Y* direction as,

(i) For left arm tip, in *X* direction,

Table I: Initial parameters

Parameter	**Value**
Robot base angle (ϕ)	0^o
Joint angle (θ_1)	30^o
Joint angle (θ_2)	35^o
Joint angle (θ_3)	30^o
Joint angle (θ_4)	35^o

Table II: Parameter values used for simulation

Parameters	**Values**	
	Right Arm	**Left Arm**
Controller stiffness (K_{tc})	1000 Nm/rad	1000 Nm/rad
Controller damping (R_{tc})	100 Nms/rad	100 Nms/rad
Controller inertia (I_c)	1 Kgm^2	1 Kgm^2
Gripper stiffness (K_g)	100 N/m	100 N/m
Gripper damping (R_g)	10 Ns/m	10 Ns/m
Virtual foundation stiffness (K_f)	1000 N/m	1000 N/m
Virtual foundation damping (R_f)	100 Ns/m	100 Ns/m
Virtual foundation mass (M_f)	10 kg	10 kg
Virtual foundation inertia (I_f)	40 kgm^2	40 kgm^2
First link mass (m_1 & m_3)	15.68 kg	15.68 kg
Second link mass (m_2 & m_4)	11.76 kg	11.76 kg
First link inertia (I_1 & I_3)	0.2153 kgm^2	0.2153 kgm^2
Second link inertia (I_2 & I_4)	0.0929 kgm^2	0.0929 kgm^2
First link length (l_1 & l_3)	0.4 m	0.4 m
Second link mass (l_2 & l_4)	0.3 m	0.3 m
Pad stiffness (K_p)	1000 N/m	1000 N/m
Pad damping (R_p)	100 Ns/m	100 Ns/m
High feed forward gain (μ)	2	2
High gain parameter (β)	2	2
Limiting gripper force (F_{lim})	40 N	-40 N *
Constant (K_{ini})	0	
Proportional gain (K_{GP})	0.1	
Integral gain (K_{GI})	0.1	
Space robot base mass (M_v)	200 Kg	
Space robot base inertia (I_v)	40 Kgm^2	
Floating body mass (M_b)	10 kg	
Floating body inertia (I_b)	1 kgm^2	
For force error integrator		
$K\tau$	100 N/m	
$R\tau$	80 Ns/m	

* Towards left

$$\dot{X}tip_L = swi(t_0, t) * A + swi(t, t_0) * R\cos(\omega t) \quad (16)$$

and in *Y* direction,

$$\dot{Y}tip_L = swi(t, t_0) * R\sin(\omega t) \quad (17)$$

(ii) For right arm tip, in *X* direction,

$$\dot{X}tip_R = -swi(t_0, t) * A + swi(t, t_0) * R\cos(\omega t) \quad (18)$$

and in Y direction,

$$\dot{Y}tip_R = swi(t,t_0) * R\sin(\omega t) \tag{19}$$

where $0 < t < \pi / \omega$, A and R are the constants.

Let us assume that the absolute frame $\{A\}$ and vehicle frame $\{V\}$ are coincident. The initial tip position for right arm is (0.5932 m, 0.4718 m) and for left arm is (-0.5939 m, 0.4715 m) of the space robot with respect to absolute frame as shown in Fig. (7).

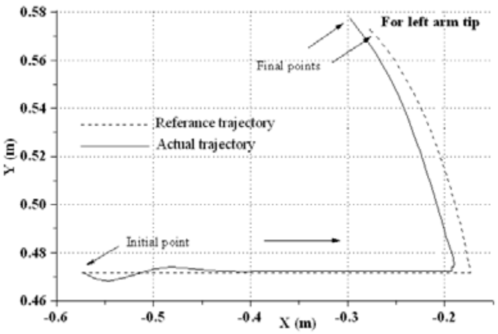

Fig. 8: Reference and actual tip displacement of space robot left arm

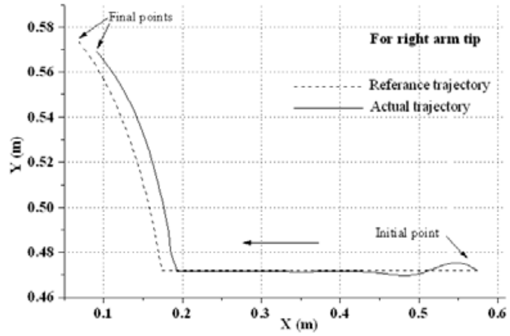

Fig. 9: Reference and actual tip displacement of space robot right arm

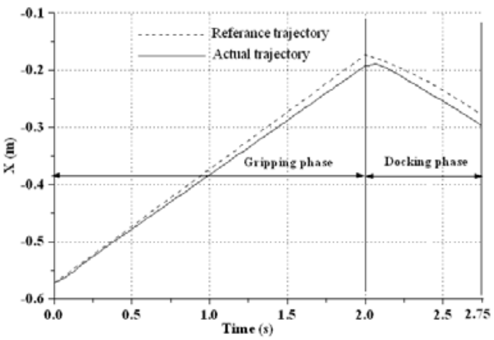

Fig. 10: Plot of tip X displacement of left arm versus time

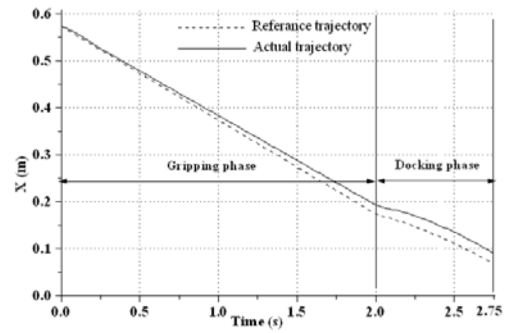

Fig. 11: Plot of tip X displacement of right arm versus time

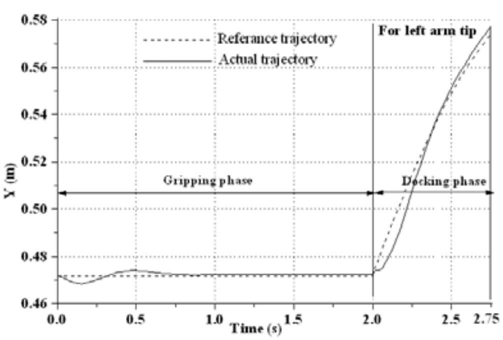

Fig. 12: Plot of tip Y displacement of left arm versus time

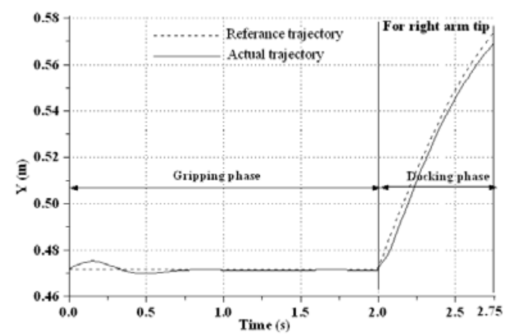

Fig. 13: Plot of tip Y displacement of right arm versus time

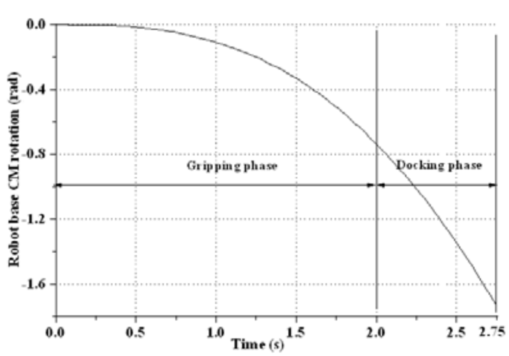

Fig. 14: Plot of the robot base rotation versus time

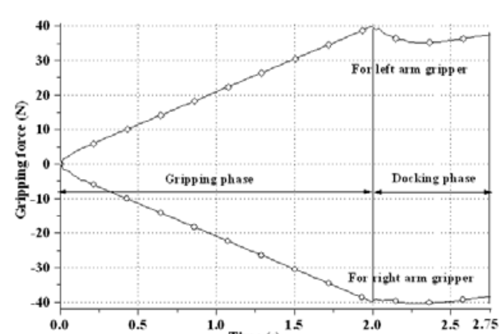

Fig. 15: Plot of gripper force generated versus time

The simulation is carried out for 2.75s in which the initial 2 s is allowed to grasp the floating body by the grippers of both the arms and remaining time is for docking of the floating body. Fig. (8) and (9) show the plots of the reference and actual tip displacement of left and right arm respectively. It is seen from these figures that the tips of both the arms closely track the reference trajectory in X and Y directions. Fig. (10) and (11) show the plots of the reference and actual tip X displacement versus time for left and right arms respectively where as Fig. (12) and (13) show the plots of the reference and actual tip Y displacement versus time for left and right arms respectively. The rotation of CM of the robot base is depicted in Fig. (14). It is seen that the robot base continuously dragged as no attitude controller device has been used here.

Fig. (15) shows the plots of the forces generated in the grippers versus time for both the arms of the space robot. It is also seen from this figure that the required value of minimum forces in both the grippers closely maintained during docking of the floating body.

5 Conclusion

In this paper, the methodology for the force control by impedance control at the interaction point between the tips of the arms of the two DOF dual arm planar cooperative space robot is illustrated. The methodology is derived by tacking analogy from a ground robot. The impedance control of a space robot is achieved by a virtual foundation. The efficiency of the scheme is demonstrated through simulation by bond graph modeling. It is observed that the controller is able to limit the interaction force within the commanded value and docking operation has been performed successfully.

Acknowledgement

Authors are thankful to Indian Space Research Organisation (ISRO) for providing necessary financial assistance to carry out the research work.

References

[1] S. Dubowsky and E. Papadopoulos, “The Kinematics, Dynamics, and Control of Free-Flying and Free-Floating Space Robotic Systems”, *IEEE transactions on Robotics and Automation*, Vol. 9, No. 5, 1993, pp 531-543.

[2] E. Papadopoulos and S. Ali A. Moosavian, “Dynamics and Control of Multi-arm Space Robots during Chase and Capture Operations”, *Proc. of the International Conference on Intelligent Robots and Systems, 1-8. Munich, Germany, September 12-16, 1994,*

[3] P. Huang, Y. Xu, and B Liang, “Dynamic Balance Control of Multi-arm Free-Floating Space Robots”, *International Journal of Advanced Robotic Systems*, Vol. 2, No. 2, 2005, pp 117 – 124.

[4] J. Yuan, C. Liu and G. Li, “Dynamics Coordinated Control Method of Multi-Arm Free-Flying Space Robot with External Force Acting”, *Proc. of the 6th World Congress on Intelligent Control and Automation, 8933-8937, Dalian, China, June 21-23, 2006.*

[5] M. Annapragada and S. K. Agrawal, “Design and Experiments on Free-Floating Planar Robot for Optimal Chase and Capture Operations in Space”, *Robotics and Autonomous Systems*, Vol. 26, 1998, pp 281-297.

[6] S. Ali A. Moosavian and R. Rastegari, “Multiple-Arm Space Free-Flying Robots for Manipulating Objects with Force Tracking Restrictions”, *Robotics and Autonomous Systems*, Vol. 54, 2006, pp 779-788.

[7] C. S. Kumar, and A. Mukherjee, “Robust Control of a Robot Manipulator on a flexible Foundation”, *Proc. of the 4th international Conference on CAD/CAM, Robotics & Factories of Future, Tata McGraw-Hill 727-742, , New Delhi, India, 1989.*

[8] Nachiket P. Deshpande, Haresh Patolia, P. M. Pathak and Satish C. Jain, “Attitude Disturbance Minimization in Space Robot using Dual Arm”, *Proc. of IEEE International Conference on Mechatronics and Automation (ICMA), 744-749, Takamatsu, Kagawa, Japan, 2008.*

[9] P. M. Pathak, A. Mukherjee and A. Dasgupta, “Impedance Control of Space Robots Using Passive Degrees of Freedom in Controller Domain”, *Transactions of the ASME*, 2005, Vol. 127, pp 564-578.

[10] C. S. Kumar, A. Mukherjee and M. A. Faruqi, “Some Finer Aspects of Impedance Modulation on Hybrid Tracking and Force controlled Manipulators”, *Proc. of International Conference on Bond Graph Modeling and Simulation (ICBGM), , 214-219. California, 1993*

[11] A. Mukherjee, R. Karmarkar, and A. K. Samantray, *Bond graph in Modeling, Simulation and Fault Identification*, I.K. International Publishing house Pvt. Ltd. 2006.

[12] Users Manual of SYMBOLS Shakti, High-Tech Consultants, S.T.E.P., Indian Institute of Technology, Kharagpur, 2006. http://www.htcinfo.com